



# Evidence for heavy fuel oil combustion aerosols from chemical analyses at the island of Lampedusa: a possible large role of ships emissions in the Mediterranean

S. Becagli<sup>1</sup>, D. M. Sferlazzo<sup>2</sup>, G. Pace<sup>3</sup>, A. di Sarra<sup>3</sup>, C. Bommarito<sup>4</sup>, G. Calzolari<sup>5</sup>, C. Ghedini<sup>1</sup>, F. Lucarelli<sup>5</sup>, D. Meloni<sup>3</sup>, F. Monteleone<sup>4</sup>, M. Severi<sup>1</sup>, R. Traversi<sup>1</sup>, and R. Udisti<sup>1</sup>

<sup>1</sup>Department of Chemistry, University of Florence, Via della Lastruccia 3, 50019 Sesto Fiorentino, Florence, Italy

<sup>2</sup>ENEA, Laboratory for Earth Observations and Analyses, 92010, Lampedusa, Italy

<sup>3</sup>ENEA, Laboratory for Earth Observations and Analyses, 00123, S. Maria di Galeria, Rome, Italy

<sup>4</sup>ENEA, Laboratory for Earth Observations and Analyses, 90141, Palermo, Italy

<sup>5</sup>Department of Physics, University of Florence and I.N.F.N., Sez. Florence, Via Sansone 1, 50019 Sesto Fiorentino, Florence, Italy

Correspondence to: S. Becagli (silvia.becagli@unifi.it)

Received: 20 October 2011 – Published in Atmos. Chem. Phys. Discuss.: 8 November 2011

Revised: 19 March 2012 – Accepted: 28 March 2012 – Published: 11 April 2012

**Abstract.** Measurements of aerosol chemical composition made on the island of Lampedusa, south of the Sicily channel, during years 2004–2008, are used to identify the influence of heavy fuel oil (HFO) combustion emissions on aerosol particles in the Central Mediterranean. Aerosol samples influenced by HFO are characterized by elevated Ni and V soluble fraction (about 80 % for aerosol from HFO combustion, versus about 40 % for crustal particles), high V and Ni to Si ratios, and values of  $V_{\text{sol}} > 6 \text{ ng m}^{-3}$ . Evidence of HFO combustion influence is found in 17 % of the daily samples. Back trajectories analysis on the selected events show that air masses prevalently come from the Sicily channel region, where an intense ship traffic occurs. This behavior suggests that single fixed sources like refineries are not the main responsible for the elevated V and Ni events, which are probably mainly due to ships emissions.

$V_{\text{sol}}$ ,  $Ni_{\text{sol}}$ , and non-sea salt  $\text{SO}_4^{2-}$  ( $\text{nssSO}_4^{2-}$ ) show a marked seasonal behaviour, with an evident summer maximum. Such a pattern can be explained by several processes: (i) increased photochemical activity in summer, leading to a faster production of secondary aerosols, mainly  $\text{nssSO}_4^{2-}$ , from the oxidation of  $\text{SO}_2$  (ii) stronger marine boundary layer (MBL) stability in summer, leading to higher concentration of emitted compounds in the lowest atmospheric layers. A very intense event in spring 2008 was studied in detail,

also using size segregated chemical measurements. These data show that elements arising from heavy oil combustion (V, Ni, Al, Fe) are distributed in the sub-micrometric fraction of the aerosol, and the metals are present as free metals, carbonates, oxides hydrates or labile complex with organic ligands, so that they are dissolved in mild condition ( $\text{HNO}_3$ , pH1.5).

Data suggest a characteristic  $\text{nssSO}_4^{2-}/V$  ratio in the range 200–400 for HFO combustion aerosols in summer at Lampedusa. By using the value of 200 a lower limit for the HFO contribution to total sulphates is estimated. HFO combustion emissions account, as a summer average, at least for  $1.2 \mu\text{g m}^{-3}$ , representing about 30 % of the total  $\text{nssSO}_4^{2-}$ , 3.9 % of  $\text{PM}_{10}$ , 8 % of  $\text{PM}_{2.5}$ , and 11 % of  $\text{PM}_1$ . Within the used dataset, sulphate from HFO combustion emissions reached the peak value of  $6.1 \mu\text{g m}^{-3}$  on 26 June 2008, when it contributed by 47 % to  $\text{nssSO}_4^{2-}$ , and by 15 % to  $\text{PM}_{10}$ .

## 1 Introduction

The lowest grade fuels (the so-called residual fuel oils or heavy fuel oils – HFO) are largely used in power plants and in marine diesel engines. They contain large concentrations of sulphur and different ash forming metals, which contribute

strongly to particle emissions (Agrawal et al., 2010). It is difficult to distinguish atmospheric particles produced by power plants or refineries and by ship engines because of the mixing of sources having similar tracers and ratios between them (Viana et al., 2009). These sources are often grouped together in various studies aimed at source apportionment of atmospheric aerosols (e.g. Amato et al., 2009; Mamanea et al., 2008). The simultaneous presence of elevated anthropic (including refineries, power plants, and an intense ship traffic) and natural emissions in the Mediterranean make this region one of the most polluted in the world (e.g., Kouvarakis et al., 2000; Lelieveld and Dentener, 2000; Marmer and Langmann, 2005). Studies on HFO combustion and ship emissions in the Mediterranean have been carried out mainly in harbour areas and coastal cities by aerosol chemical analysis and source apportionment (Pandolfi et al., 2011; Viana et al., 2009; Mazzei et al., 2008). Assessment studies on the role of ship emissions in the Mediterranean basin are so far based on inventories and model analyses (e.g., Marmer et al., 2009; Olivier et al., 2005; Eyring et al., 2005; Vestreng et al., 2007) and show that the contribution of ships to air pollution in the Mediterranean atmosphere is significant, although its quantification strongly dependent on the used emission inventory. The verification of ship emission inventories, and particularly those in the open sea, against observations is a difficult task due to lack of continuous measurements over the open sea and to the complex involved atmospheric processes.

In this context, studies performed in open sea far from source of HFO combustion other than ships, are relevant in order to investigate the current impact of the ship emissions on the formations of primary and secondary aerosol, and how the predicted future growth of ship traffic and the geographical expansion of waterways and ports, possibly combined with international regulations, are going to affect the atmospheric composition.

Although shipping contributes significantly to the international transportation sector, its emissions are not well quantified and are one of the least regulated anthropogenic sources (IMO, 2008; Cofala et al., 2007). Several studies point towards the need of international regulations on ship emissions, as those active in Europe, where the land based emissions of sulphur have been successfully reduced since 1980's.

Recently, several studies (Petzold et al., 2008; Moldanova et al., 2009; Lack et al., 2009; Agrawal et al. 2008a, b, 2010) reported chemical, physical, and optical properties of emitted particles and gases by analyzing plumes of a large number of commercial shipping vessel, also considering different engines load condition. These studies provide the emission factors of various gases (carbon monoxide, nitrogen oxides, sulphur dioxide, carbon dioxide), chemical compounds in the particulates (S, metals), and aerosol mass emitted from marine engines fed with heavy fuel oil.

Gases and particles emitted by ship and other HFO combustion impact human health (Corbett et al., 2007), influence

acidification and eutrofization of water and soil in coastal regions due to deposition of sulphur and nitrogen compounds (Derwent et al., 2005), and affect climate through sulphur containing particles (Devasthale et al., 2006; Lauer et al., 2007), greenhouse gases (Stern, 2007), and absorbing black carbon aerosols (Lack et al., 2009). Moreover, sulphate aerosol has an indirect climate effect influencing cloud structure and properties (e.g., Conover, 1966; Coakley and Walsh, 2002)

The present paper presents the first experimental identification and quantification of  $\text{SO}_4^{2-}$  from HFO combustion aerosol based on chemical analyses of  $\text{PM}_{10}$  samples collected at the island of Lampedusa in the central Mediterranean Sea.

## 2 Measurements and methods

The measurements were carried out at the Station for Climate Observations, maintained by ENEA (the national Agency for New Technologies, Energy, and Sustainable Economic Development of Italy) at Lampedusa (35.5° N, 12.6° E). Lampedusa is a small island in the Central Mediterranean sea far at least 100 km from the nearest Tunisian coast. At the Station for Climate Observations, which is located on a 45 m a.s.l. plateau on the North-Eastern coast of Lampedusa, continuous observations of greenhouse gases concentration (Artuso et al., 2009, 2010), aerosol properties (di Sarra et al., 2011; Meloni et al., 2006; Pace et al., 2006), total ozone, ultraviolet irradiance (di Sarra et al., 2002; Meloni et al., 2004; Di Biagio et al., 2010), and other climatic parameters are carried out.

In this study we will use aerosol optical properties measured with a multi-filter rotating shadowband radiometer (MFRSR), and chemical analyses of sampled aerosols on filters.

The MFRSR (Harrison et al., 1994) is a seven-channel radiometer which measures global and diffuse irradiances, and allows the determination of column aerosol optical depth at 5 wavelengths (416, 496, 615, 671, and 869 nm). The measurement details and data retrieval is described by Pace et al. (2006).

The aerosol sampling was started in June 2004 at daily resolution, alternating in sequence sampling of  $\text{PM}_{10}$ ,  $\text{PM}_{2.5}$ , and  $\text{PM}_{1.0}$  (particulate matter with aerodynamic diameter lower than 10, 2.5 and 1.0  $\mu\text{m}$  respectively). Only the  $\text{PM}_{10}$  sampling head at daily resolution was used since 2007. During the sampling period some interruptions occurred due to technical failures. Here results on the chemical composition of  $\text{PM}_{10}$  are reported. The sampler was loaded with 47 mm diameter 2  $\mu\text{m}$  nominal porosity Teflon filters. The filters were weighted before and after sampling in order to obtain the mass of the collected atmospheric particulate. All filters were conditioned for at least 24 h prior to weighing at a relative humidity of 35–45 % and temperature of 25°C.

A quarter of each Teflon filter was extracted using MilliQ water (about 10 ml, accurately evaluated by weighing) in ultrasonic bath for 15 min, and the ionic content was evaluated by ion chromatography. Every sample was analysed for cations ( $\text{Na}^+$ ,  $\text{NH}_4^+$ ,  $\text{K}^+$ ,  $\text{Mg}^{2+}$ ,  $\text{Ca}^{2+}$ ), inorganic anions ( $\text{F}^-$ ,  $\text{Cl}^-$ ,  $\text{NO}_3^-$ ,  $\text{SO}_4^{2-}$ ), and some organic anions (methanesulphonate – MSA, acetate, formate, glycolate, oxalate) as reported in Becagli et al. (2011).

Another quarter was extracted in ultrasonic bath for 15 min with MilliQ water acidified at pH 1.5–2 with ultrapure nitric acid obtained by sub-boiling distillation. This extract was used for determination of the soluble part of metals by Inductively Coupled Plasma Atomic Emission Spectrometer (ICP-AES, Varian 720-ES) equipped with an ultrasonic nebulizer (U5000 AT<sup>+</sup>, Cetac Technologies Inc.). Samples have been spiked with 100 ppb of Ge used as internal standard ( $\lambda = 209.4$  nm), and calibration standards were prepared by gravimetric serial dilution from mono standards at  $1000 \text{ mg L}^{-1}$ . The value of pH was chosen because it is the lowest values found in rainwater (Li and Aneja, 1992) and leads to the determination of the metals fraction more available for biological organisms. Filters field blanks show V and Ni soluble fractions (hereafter  $V_{\text{sol}}$  and  $Ni_{\text{sol}}$ ) concentrations below the detection limits ( $0.04 \text{ ng m}^{-3}$  and  $0.09 \text{ ng m}^{-3}$ , respectively) in working conditions.

The remaining half filters were analysed for the total (soluble + insoluble) elemental composition by the proton induced X ray emission (PIXE) technique (Calzolari et al., 2006; Lucarelli et al., 2011). The PIXE analysis was carried out for a reduced number of samples, therefore, the elemental composition is available for a restricted data set. In addition, the amount of V was in several cases below the minimum detection limit (MDL) of the PIXE technique.

Additional sampling with an 8 stage impactor equipped with Teflon back-up filter was performed in Lampedusa in the period 17 May–20 June 2008. Half of each filter was used to determine the ionic composition, while the other half was used to measure the metals soluble fraction content with the same methodology above described.

## 3 Results

### 3.1 Identification of heavy oil combustion aerosols: chemical composition

#### 3.1.1 Vanadium and nickel

Sulphur is the dominant element in the exhausts of heavy fuel oil combustion, followed by V and Ni (Agrawal et al., 2008a). These metals are also present as minor constituents in the Earth crust, whose main component is Si (66.6% as  $\text{SiO}_2$  in the upper continental crust; Henderson and Henderson, 2009); in the upper continental crust the V/Si and Ni/Si ratio are  $3.1 \times 10^{-4}$  w/w and  $1.5 \times 10^{-4}$  w/w, respec-

tively, while the mean V/Ni ratio is 2.06 w/w (Henderson and Henderson, 2009). Heavy oil is enriched in V and Ni content with respect to the crust, and these metals are generally used as markers of HFO combustion in all size fractions of the atmospheric particulate. Different authors (Mazzei et al., 2008; Viana et al., 2009; Pandolfi et al., 2011) report characteristic values of V/Ni between 2.5 and 3.5 for ships emissions. These values are obtained by applying statistical approaches (Positive Matrix Factorization) to an extensive chemical data set of aerosol sampled near harbours in the Mediterranean Sea. A relatively wide range of V/Ni ratio (2.3–4.5) was measured by direct sampling at the exhausts of different auxiliary ship engines fed by different fuels (Nigam et al., 2006), and from the main propulsor ship engine at different speed mode (Agrawal et al., 2008a and b). V/Ni = 3 was found from power plant and oil refinery emissions (Pandolfi et al., 2011).

Given the small difference between the typical V/Ni ratios for HFO combustion aerosol and for dust, these two sources cannot be easily separated on the basis of this ratio.

#### 3.1.2 V and Ni enrichment with respect to crustal sources

Since the V/Ni ratio does not allow an unequivocal attribution to the HFO combustion source, we use Si, which is used, when analytically determined, as the main marker for crust to identify and remove from the dataset samples with a significant crustal contribution.

Elevated Si levels might be associated, in addition to crustal particles, also to fly ash from high temperature combustion processes, mainly from coal electric power plants (Gaffney and Marley, 2009). However, the contribution of fly ash to  $\text{PM}_{10}$  is negligible (Gaffney and Marley, 2009) and Si, Al, and Fe elements are commonly used to identify and quantify the crustal content, particularly in the Mediterranean region (e.g. Remoundaki et al., 2011; Koçak et al., 2007; Nicolás et al., 2008).

Peaks of V and Ni are expected when HFO combustion or crustal particles are sampled; the two sources are characterized by different Si content, low for the anthropic (HFO combustion), high for the natural (crustal). Thus, we used the Ni/Si and V/Si ratios to distinguish between V and Ni due to heavy oil combustion and to crustal sources. Ni and V determined by PIXE (i.e. their total content) was used for Ni/Si and V/Si ratios calculation. The ratios between the measured Ni/Si or V/Si and the typical corresponding crustal ratios, defined as enrichment factors, are used to identify crustal samples. Following previous studies (e.g., Adams et al., 1980; Chester et al., 2000), samples with an enrichment value  $< 10$  are assumed to correspond with cases influenced by the crustal source, while an enrichment value  $> 10$  identifies cases dominated by non-crustal sources (anomalously enriched elements), and in particular heavy oil combustion.

**Table 1.** Correlation parameters between V and Ni soluble and total fractions for ship aerosol cases ( $V_{\text{sol}} > 6 \text{ ng m}^{-3}$ ) and for Saharan dust cases ( $\text{Si} > 925 \text{ ng m}^{-3}$  and  $V_{\text{sol}} < 6 \text{ ng m}^{-3}$ ).

	Slope ( $\pm$ error)	$R^2$	n.
$V_{\text{sol}}/V_{\text{tot}}$ ship events	0.80 ( $\pm 0.02$ )	0.932	113
$V_{\text{sol}}/V_{\text{tot}}$ pure Saharan dust events	0.36 ( $\pm 0.02$ )	0.798	68
$\text{Ni}_{\text{sol}}/\text{Ni}_{\text{tot}}$ ship events	0.77 ( $\pm 0.02$ )	0.939	113
$\text{Ni}_{\text{sol}}/\text{Ni}_{\text{tot}}$ pure Saharan dust events	0.45 ( $\pm 0.02$ )	0.787	114

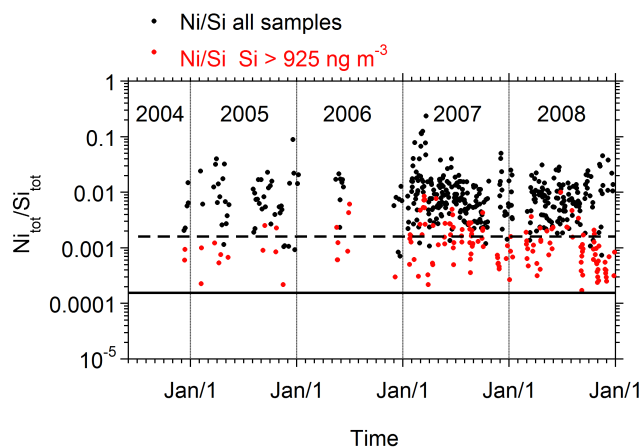


**Fig. 1.** Temporal evolution of  $\text{Ni}_{\text{tot}}/\text{Si}_{\text{tot}}$  in  $\text{PM}_{10}$  samples collected at Lampedusa island. Black line represent the Ni/Si mean ratio in upper continental crust (Henderson and Henderson, 2009), dashed line represent the threshold values for sharing samples enriched (one order of magnitude higher than black line). Red dots are samples with high dust content ( $\text{Si} > 925 \text{ ng m}^{-3}$ ).

Figure 1 shows the daily values of Ni/Si derived from PIXE measurements ( $\text{Ni}_{\text{tot}}/\text{Si}_{\text{tot}}$ ). The  $\text{Ni}_{\text{tot}}/\text{Si}_{\text{tot}}$  ratio is 10 times higher than the value for crustal particles (dashed line in Fig. 1) in 79 % of the measured samples. A higher fraction of enriched samples is obtained for the  $V_{\text{tot}}/\text{Si}_{\text{tot}}$  ratio (88 % of the samples are enriched in V). The V total content was determined in a minor number of samples than Ni because there are cases with V below the PIXE detection. As a consequence, the fraction of data with elevated ratio is higher for V/Si than for Ni/Si.

Most of the not enriched samples belongs to days in with  $\text{Si} > 925 \text{ ng m}^{-3}$ ; this value corresponds to the 75th percentile of the distribution of occurrence of Si concentration. Previous studies carried out on the basis of aerosol optical depth measurements show that dust is present at Lampedusa in about 26 % of the days (Meloni et al., 2007). Cases with  $\text{Si} > 925 \text{ ng m}^{-3}$  correspond to moderate and high dust conditions at Lampedusa, and identify cases which are evidently affected by the crustal component. Back trajectories (not shown for brevity) confirm that the air masses originate from or pass over the Sahara desert before reaching Lampedusa in days with concentration of  $\text{Si} > 925 \text{ ng m}^{-3}$ .

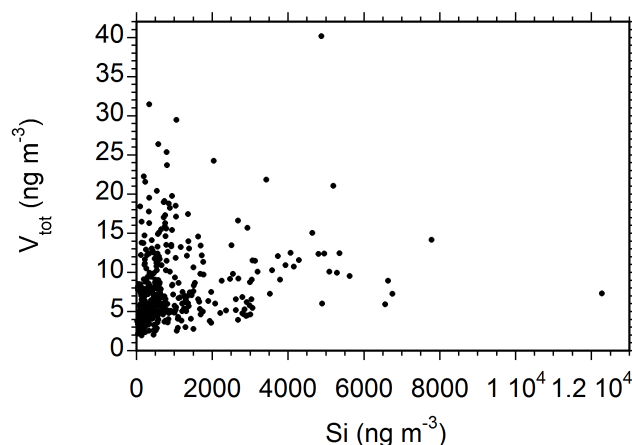


**Fig. 2.** Scatter plot of V total content obtained by PIXE versus Si.

Figure 2 shows the scatterplot of daily total content of V versus Si (blue dots). In general, dust-laden samples show a relatively small amount of V, suggesting that cases with elevated values of V have a different source with respect to Si.

### 3.1.3 V and Ni solubility

The measured concentrations of  $V_{\text{sol}}$  and  $\text{Ni}_{\text{sol}}$  for the non-enriched events are lower than for the enriched cases, and are always below 8 and  $2.6 \text{ ng m}^{-3}$ , respectively. Only 6 events (less than 5 % of the dataset) are in the range  $6\text{--}8 \text{ ng m}^{-3}$  for V, and  $2.3\text{--}2.6 \text{ ng m}^{-3}$  for Ni. The threshold of  $6 \text{ ng m}^{-3}$  (hereafter  $V_{\text{st}}$ ) for  $V_{\text{sol}}$  is chosen to identify HFO combustion enriched samples on the basis of measurements of  $V_{\text{sol}}$ .

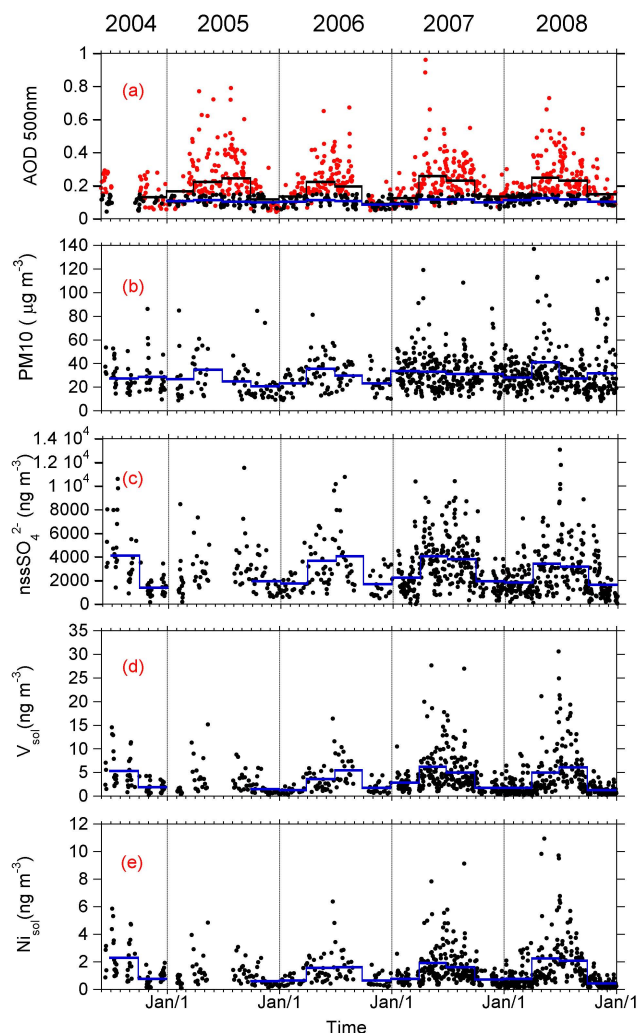
The V and Ni solubility appears to depend on the originating source. By plotting  $V_{\text{sol}}$  and  $\text{Ni}_{\text{sol}}$  versus the total V and Ni, respectively, we obtain two different behaviours: the HFO combustion enriched cases ( $V_{\text{sol}} > 6 \text{ ng m}^{-3}$ ) display a larger slope, thus a higher solubility than during Saharan dust events ( $\text{Si} > 925 \text{ ng m}^{-3}$  and  $V_{\text{sol}} < 6 \text{ ng m}^{-3}$ ). Table 1 reports slopes and regression coefficients for the various plots. In the events classified as influenced by the anthropic source both V and Ni are easily dissolved (the soluble fraction is 80 % and 77 % for V and Ni, respectively) in the mild extraction condition ( $\text{HNO}_3$  – pH 1.5) because they are mainly present as free metals, oxides hydrates, or

organo-metal compounds. Sippula et al. (2009) report that several soluble compounds such as sodium vanadates and nickel hydroxides are formed during HFO combustion. On the contrary, the presence of V and Ni in the silica matrix or as oxides in samples with high dust content is expected to produce a lower solubility, as it is found in our samples (36% and 45% for V and Ni, respectively). Consequently, samples influenced by heavy oil combustion have a higher content of  $V_{\text{sol}}$  and  $Ni_{\text{sol}}$ , which are present in the available form for biological organisms, and are more capable to exert toxicity.

### 3.1.4 Sulphate and PM<sub>10</sub> concentration

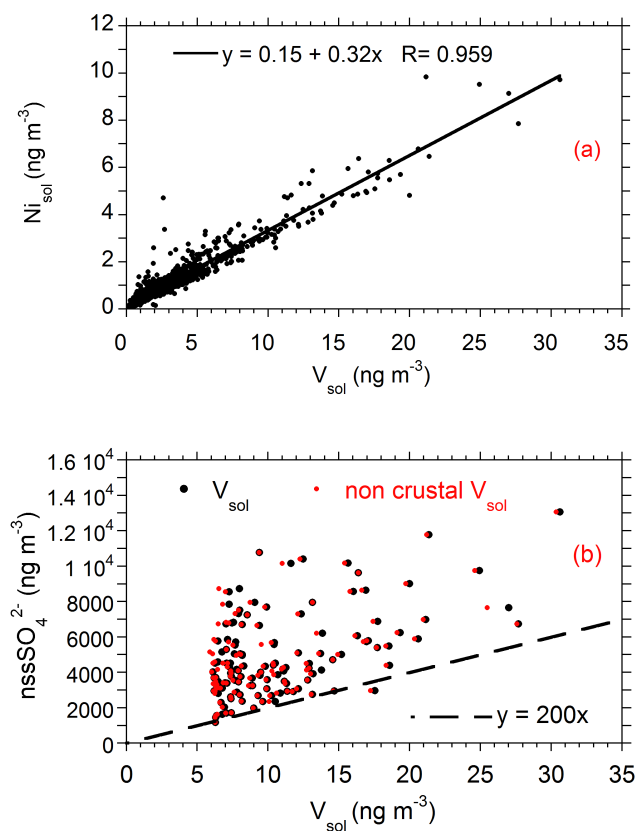
Figure 3 shows the temporal evolution of the daily average aerosol optical depth (AOD) at 500 nm, of the daily PM<sub>10</sub> mass concentration, and of the main markers of heavy fuel oil: non sea salt sulphate ( $\text{nssSO}_4^{2-}$ ),  $V_{\text{sol}}$  and  $Ni_{\text{sol}}$  from PM<sub>10</sub> samples collected at Lampedusa in the period June 2004–December 2008. Three-month averages of the measured parameters are also shown to emphasize the seasonal evolution. Cases in which the measured AOD is strongly influenced by Saharan dust are also reported in the figure (red dots in Fig. 3a). The method by Pace et al. (2006), based on the measured values of AOD and Ångström exponent and on the analysis of the backward trajectories, was used for the identification of cases with large Saharan dust contribution to the AOD. Since the AOD provides information on the entire air column, the identification of a Saharan dust case does not necessarily imply that mineral particles are present close to the surface.

Figure 3 shows a marked seasonal pattern with spring–summer maxima of the AOD and of the trace chemical markers. As discussed by Di Iorio et al. (2009), the dust optical depth and vertical distribution show a large seasonal cycle, with elevated AOD and a wider vertical extension in spring and summer; the seasonal change is mainly controlled by dust transport occurring over the boundary layer. On the contrary, non dust cases and boundary layer aerosols display a very limited seasonal change (black dots and blue line in Fig. 3a), as it is also confirmed by the PM<sub>10</sub> measurements (Fig. 3b). The PM<sub>10</sub> concentration reaches elevated values, up to about  $140 \mu\text{g m}^{-3}$ , mainly in spring; also the highest peaks in AOD in 2007 and 2008, close to 1, occur in spring. The highest peaks in PM<sub>10</sub> and AOD are due to Saharan dust events, and will not be discussed in detail here. Elevated values and isolated peaks of  $V_{\text{sol}}$ ,  $Ni_{\text{sol}}$ , and  $\text{nssSO}_4^{2-}$  are observed throughout spring–summer and especially in June–July. A scatter plot of  $Ni_{\text{sol}}$  versus  $V_{\text{sol}}$ , and of  $\text{nssSO}_4^{2-}$  versus  $V_{\text{sol}}$  for cases in which the anthropic contribution is relevant (i.e.  $V_{\text{sol}} > 6$ ) is shown in Fig. 4.  $V_{\text{sol}}$  and  $Ni_{\text{sol}}$  are closely related, suggesting that the two species originate from the same source. The slope of the linear regression between  $V_{\text{sol}}$  and  $Ni_{\text{sol}}$  for the cases classified as influenced by HFO combustion ( $R^2 = 0.978$ ) is  $2.98 \pm 0.04$ , in agreement with previous studies (Mazzei et al., 2008; Agrawal et al.,



**Fig. 3.** Temporal evolution of AOD, PM<sub>10</sub>,  $\text{nssSO}_4^{2-}$ ,  $V_{\text{sol}}$  and  $Ni_{\text{sol}}$ , at Lampedusa island. Blue lines in plot (b), (c), (d), and (e) represent the three months mean. Red dots in the plot (a) are related to Saharan dust events chosen as  $\text{AOD} > 0.15$  and  $a < 0.5$  (Pace et al., 2006). Black dots represent the remaining days. In this plot the dark line represent the AOD three month average, the blue one the three month mean excluding the Saharan dust event (i.e. calculated over the black dot).

2008a and b, Viana et al. 2009; Pandolfi et al., 2011). A very good correlation ( $R^2 = 0.945$ ) is also found for events influenced by crustal particles; the slope of the linear fit is lower ( $2.54 \pm 0.05$ ) than for the HFO combustion cases, and somewhat higher than the mean V/Ni crustal ratio (2.06). Cases of mixing between crustal and anthropogenic particles might explain this behaviour. It must be pointed out that Viana et al. (2009) found in some Saharan cases very high V/Ni ratios, up to about 12; although we do not find such high values, mixing of crustal particles of different V/Ni ratio may also play a role.



**Fig. 4.** Scatter plots  $Ni_{sol}$  (a) and  $nssSO_4^{2-}$  (b) vs.  $V_{sol}$ . Line in plot a represents the linear correlation, dashed line in (b) represents the ratio  $nssSO_4^{2-}/V_{sol} = 200$ . Red dots in (b) represent non crustal  $V_{sol}$ .

The limited difference found between the slopes for HFO combustion and crustal samples confirms that the  $V/Ni$  ratio alone does not allow to separate the two sources.

The behaviour of non-sea salt sulphate does not appear to be closely linked to  $V_{sol}$  and  $Ni_{sol}$ . Beside heavy fuel oil combustion, several other sources (anthropogenic origin from long range transport, marine biogenic, crustal, volcanic) contribute to the non sea salt sulphate in the Central Mediterranean Sea. For this reason  $V_{sol}$  and  $nssSO_4^{2-}$  are not directly coupled, and the quantification of  $SO_4^{2-}$  contribution from HFO combustion emissions to the  $nssSO_4^{2-}$  total budget is a difficult task.

### 3.2 Identification of heavy oil combustion aerosols: trajectory analysis

The chemical aerosol composition was related to air mass trajectories with the aim of identifying main source regions.

Back-trajectories were calculated using local wind data measured at the Lampedusa Station for Climate Observations on a 10 m tall mast with a time resolution of 10 min, assuming that the wind along the back trajectory is at each

time step equal to the one measured at the same time at Station. Lampedusa is a small island, far more than 100 km from the nearest coast, and we assume that the wind measured at Lampedusa is representative for a relatively wide region. The main advantage of this method is the direct use of high temporal resolution measurements. The objective of the trajectory analysis is to derive information on the air mass origin in the surrounding of Lampedusa and in a short time interval (generally up to 12 h). We expect that the reliability of the method rapidly decreases with time, and in proximity of the coasts or over land.

Backtrajectories were calculated also with the Hysplit model (Draxler and Rolph, 2012; Rolph, 2009) using the NCEP reanalysis data ( $2.5^\circ \times 2.5^\circ$  spatial and 6 h temporal resolution) during selected periods. The two approaches show very similar results. However, we believe that in the proximity of Lampedusa and for the considered limited time interval our methodology produces more detailed results, especially for cases of low wind velocity and fast changing conditions, because of the difficulty of models in reproducing the wind field close to the surface and the low temporal resolution of the reanalysis. Twelve-hour long trajectories are in most cases suited to investigate the area surrounding Lampedusa, and a broad temporal interpolation between successive model analyses is required for the HYSPLIT trajectory calculation.

Figure 5 shows 18-h long trajectories arriving at Lampedusa at the middle of the PM sampling interval. Trajectories are grouped in three-month periods, and plotted separately for cases with  $V_{sol} < 6 \text{ ng m}^{-3}$  and  $V_{sol} > 6 \text{ ng m}^{-3}$ . Similar results are found by using 12-h or 24-h trajectories. Trajectories were also calculated for different arrival times, at the beginning or at the end of the PM sampling interval. Except than in few cases, no substantial changes in the trajectory pattern are found.

The origin of the air masses corresponding to  $V_{sol} < V_{st}$  reflects the overall wind direction statistics at Lampedusa, without specific preferred directions (22 % of cases wind originates from N-NW; all the other directions show frequencies of occurrence between 2 % and 5 %). The air masses showing evidence of HFO combustion aerosol influence display a strong dependency on the originating direction: they are mostly of Northern origin, and passed over the Strait of Sicily, i.e. in correspondence with the main maritime route crossing the Mediterranean sea from the Strait of Gibraltar to the Suez Canal. 26.5 % (35) of the cases with  $V_{sol} > V_{st}$  correspond to air masses coming from a narrow direction ( $345^\circ \pm 7.5^\circ$ ); 63.6 % (84) of the cases correspond to air masses originating between  $322.5^\circ$  and  $37.5^\circ$ . The same region also includes 80.8 % of the cases with  $V_{sol} > 10$  (52 cases). Trajectories with  $V_{sol} > V_{st}$  do not show any significant dependency on the wind intensity (the mean wind intensity along the back trajectory ranges from 1.5 to  $11 \text{ m s}^{-1}$ ).

The main shipping route through the Sicily channel runs about 180 km North of Lampedusa and the good correspondence between the air mass origin and the Mediterranean

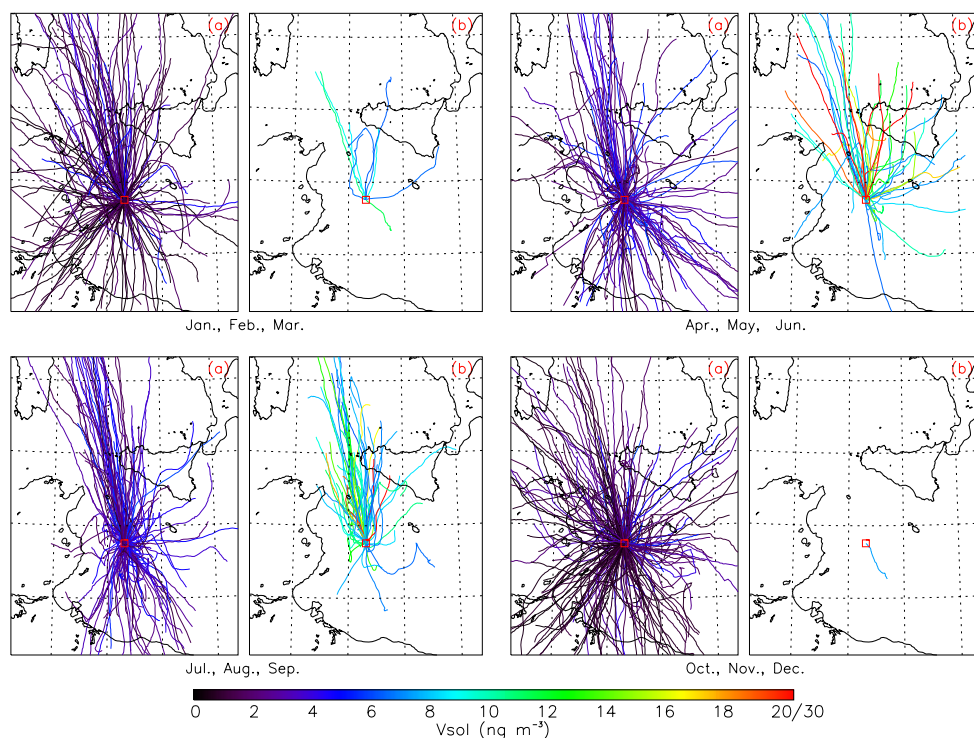


**Fig. 5.** Panels (a) and (b) show the 18 h back trajectory relatives to the measurements of  $V_{\text{sol}}$  less than or great/equal to  $6 \text{ ng m}^{-3}$  (i.e.  $V_{\text{st}}$ ) respectively. The trajectories are grouped in quarters, each one representing three months.

**Table 2.** For the two periods having different resolution time (June 2004 and August 2007) are reported: the number of PM samples (measurements of  $V_{\text{sol}}$ ), the number (frequency occurrence on the total number of annual  $V_{\text{sol}}$  measurements) of measurements with  $V_{\text{sol}} > 6 \text{ ng m}^{-3}$ , the mean and standard deviation values. The number of episodes of single and consecutive days (frequency occurrence on the number of annual  $V_{\text{sol}}$  measurements affected by ship emission) of  $V_{\text{sol}} > 6 \text{ ng m}^{-3}$ , the correspondent periods mean and standard deviation values of the single and multiple day episodes are also presented.

Year	Number of PM ( $V_{\text{sol}}$ ) samples	Number of $V_{\text{sol}} > 6 \text{ ng m}^{-3}$ measurements, annual occurrence, mean and std values	Number of episodes single or consecutive days with $V_{\text{sol}} > 6 \text{ ng m}^{-3}$ , daily annual occurrence, mean and std values				
			single day	2 days	3 days	4 days	5 days
2004–2006	241 (235)	28 11.9 % $9.7 \pm 2.8$	20 episodes 71.4 % $8.1 \pm 2.8$	1 episode 7.1 % $13.9 \pm 1.0$	2 episodes 21.4 % $10.1 \pm 2.0$		
2007–2008	594 (549)	104 18.9 % $11.0 \pm 5.3$	31 episodes 29.8 % $8.2 \pm 2.5$	8 episodes (15.4 %) $12.7 \pm 4.6$	10 episodes (28.8 %) $9.2 \pm 3.1$	3 episodes (11.5 %) $16.9 \pm 8.4$	3 episodes (14.4 %) $13.4 \pm 5.4$

main route of large vessels suggests that most of the events characterised by  $V_{\text{sol}} > 6 \text{ ng m}^{-3}$  are directly influenced by ship emissions. Figure 6 shows a statistic of the number of cases with  $V_{\text{sol}} < 6 \text{ ng m}^{-3}$  and  $V_{\text{sol}} > 6 \text{ ng m}^{-3}$  for different originating trajectory directions. Data are displayed for April–May–June, and July–August–September, separately; only two quarterly statistics are shown because the few HFO combustion aerosols events measured in autumn and winter. Evidently, as also appears in Fig. 5, air masses coming from the Sicily Channel during autumn and winter do not neces-

sarily show elevated values of  $V_{\text{sol}}$ , suggesting that transport from north north-west is required, but is not sufficient to determine high concentration of HFO combustion aerosol; different processes probably play a role in the observed seasonal evolution.

### 3.3 Seasonal evolution

As shown in Fig. 3,  $V_{\text{sol}}$ ,  $\text{Ni}_{\text{sol}}$ , and  $\text{nssSO}_4^{2-}$  display a large seasonal cycle, with a marked maximum in spring–summer. Three-month averages of the different parameters displayed

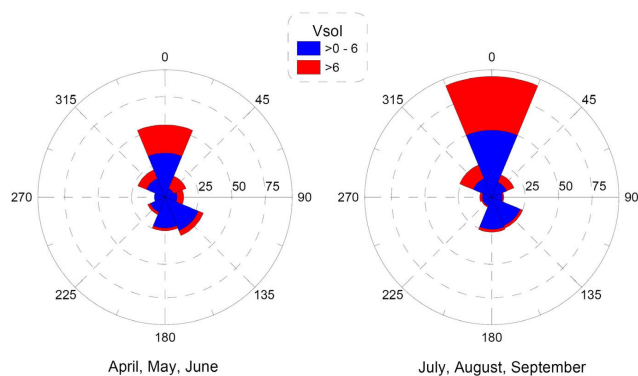


**Fig. 6.** Number of cases with  $V_{\text{sol}} < 6 \text{ ng m}^{-3}$  (blu regions) and  $V_{\text{sol}} > 6 \text{ ng m}^{-3}$  (red regions) for different originating directions of the corresponding airmass trajectories for April-May-June (left), and July-August-September (right).

in Fig. 3 were drawn to highlight their seasonal evolution. The yearly evolution of the three-month averages of  $V_{\text{sol}}$  and  $\text{nssSO}_4^{2-}$  appear remarkably similar, suggesting that, although the sources may not be coupled, they may partly respond to similar mechanisms. As discussed above, the seasonal behaviour is not due to a significant change in the dynamical patterns and to more frequent trajectories from HFO combustion sources. Different processes thus contribute to produce this seasonal cycle.

Production of secondary aerosol is influenced by solar radiation. This effect is well known for the formation of  $\text{nssSO}_4^{2-}$ , which is derived from oxidation of  $\text{SO}_2$  by OH (see, e.g., Barbu et al., 2009). In its turn, the OH production is linked to elevated levels of ultraviolet radiation. The central Mediterranean is characterized by elevated levels of UV radiation in summer, and high ozone photolysis and OH production (e.g., Casasanta et al., 2011). Consequently,  $\text{SO}_2$  conversion into  $\text{SO}_4^{2-}$  is expected to be faster in summer. Ault et al. (2010), in a recent study found V and  $\text{SO}_4^{2-}$  in single aerosol particles from fuel combustion; they found that  $\text{SO}_4^{2-}$  is in higher concentration than in particles not containing V and suggest a catalytic effect of V on the oxidation of  $\text{SO}_2$  to  $\text{SO}_4^{2-}$ . In this process the metals would be involved in the secondary aerosol formation, favoured by high level of solar radiation.

The structure of the planetary boundary layer is expected to play a role in producing the observed seasonal cycle. Song et al. (2003) used a Lagrangian photochemical box model for an air parcel emitted from ship in the marine boundary layer. They found that conditions favouring the stability of the marine boundary layer produce a larger increase in the  $\text{SO}_2$  and sulphate concentrations than an increased emission of  $\text{SO}_2$ . The marine boundary layer is generally more stable in summer than in winter (e.g., Dayan et al., 1989), and this effect may produce elevated concentrations of sulphate and metals during this season.

Also the variability of the traffic ship may play a role in determining the observed annual cycle. Recent modeling studies which used different ship emission inventories assumed a constant source throughout the year (e.g., Marmer and Langmann, 2005; Jonson et al., 2009), explicitly because of lacking information. For instance, Marmer and Langmann (2005) found mean concentrations of sulphate aerosol almost four times higher in summer than in winter in the lowest level of their model. A limited information is available on the seasonal variability of the ship traffic in the Mediterranean, and only for selected regions (e.g., Tzannatos, 2010; ORTC, 2011). Seasonal changes in the ship traffic appear to be primarily connected with touristic activities/passenger transport, and mainly interest specific coastal areas (e.g., the Ligurian sea, several routes in Greece, etc.). The emissions from the passenger ships are however estimated to be small (Jonson et al., 2009), and probably produce a limited effect on the seasonal distribution of the emissions.

Table 2 presents some statistics on  $V_{\text{sol}}$  measurements and the cases of consecutive days with  $V_{\text{sol}} > V_{\text{st}}$ . The whole database extends over 5 yr, but only the last 2 yr are characterised by regular daily samples. As shown in Table 2, from 2004 to 2006 there are a total of 235  $V_{\text{sol}}$  measurements (i.e. yearly number of measurements varying between 66 and 91), and only about 12 % of the cases presents  $V_{\text{sol}} > V_{\text{st}}$ . The number of HFO combustion aerosol events with duration of more than one day is largest in summer.

The representativeness of 2007 and 2008 is definitely larger than in previous years, with a total of 549 daily measurements of  $V_{\text{sol}}$ . Thus we believe that results for 2007–2008, with about 19 % of cases with  $V_{\text{sol}} > V_{\text{st}}$  is more representative for the normal situation at the Lampedusa.

A simple statistics on HFO combustion events lasting more than one day is reported in Table 2. The number of cases lasting more than one day is larger in 2007–2008 (70.2 % of the cases last between 2 and 5 consecutive days) than in the 2004–2005 period (28.6 %); however, results for 2004–2006 are biased, since  $\text{PM}_{10}$  samples were not taken continuously. This effect tends to produce an underestimate of the influence of HFO combustion events in 2004–2006. Moreover, most of the episodes lasting more than one day show mean  $V_{\text{sol}}$  values larger than the mean  $V_{\text{sol}}$  of the single day cases, suggesting a progressive increase of the HFO combustion aerosol load in specific situations, leading to a strong intensity of episodes lasting for more than one day.

### 3.4 The June-July 2008 event: trajectory analysis

Figure 7 shows the back trajectories of a particular long lasting (20 days) and interesting event in which the HFO combustion influence on the aerosol chemical composition was observed to occur almost continuously from 20 June to 9 July, 2008. Elevated values of  $V_{\text{sol}}$  were measured throughout the period;  $V_{\text{sol}}$  decreased below  $V_{\text{st}}$  during only 3 days.



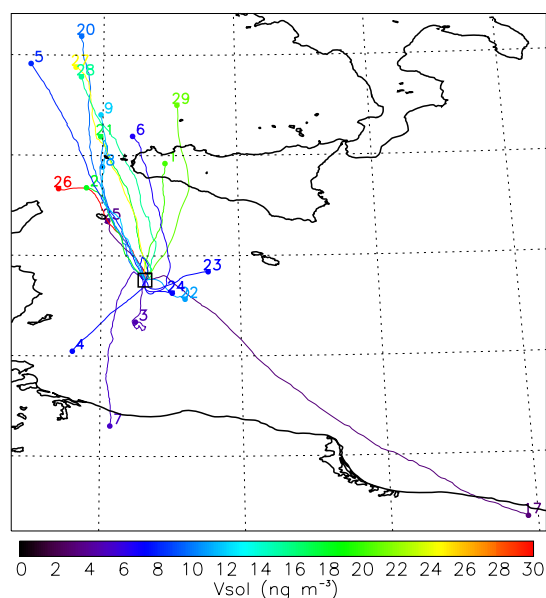


**Fig. 7.** 18-h back trajectories for the 20 June–9 July 2008 period, when only 3 daily  $V_{\text{sol}}$  measurements (25 June, 3 and 7 July) were below  $V_{\text{st}}$ . The 24-h back trajectory of 17 May is also presented. The number at the end of each back-trajectories indicates the corresponding day of June and July.

At the beginning of the event (20 and 21 June) the wind intensity decreased and advected air from the middle of the Sicily channel. From 22 to 24 June there is a notable reduction of the wind intensity, and easterly winds. On 25 June the wind was again coming from North-West, and values of  $V_{\text{sol}} < V_{\text{st}}$  were measured. From 26 June to 2 July  $V_{\text{sol}}$  reached very high values, including the maximum value of the whole dataset ( $30.6 \text{ ng m}^{-3}$ ) on 26 June; 4 out of the 7 values of  $V_{\text{sol}} > 20 \text{ ng m}^{-3}$  of the dataset occurred between 26 June and 1 July. In this period the air mass came from North, progressively shifting from Northwest to Northeast. A change of the wind direction led to Southern local air masses and  $V_{\text{sol}} < V_{\text{st}}$  on 3 July. With the exception of the back trajectory of 7 July, when southern air mass induced a low value of  $V_{\text{sol}}$ , the period ends with a recovery of the Northerly air mass flow, still inducing high values of  $V_{\text{sol}}$ .

This long extended period with strong influence from HFO combustion, and very likely ship emissions, confirms that the origin of the air masses plays a central role. In particular, the strait of Sicily seems to be the main source region. Moreover, very low winds connected with stagnant conditions are not responsible for elevated values of  $V_{\text{sol}}$ , confirming that high  $V_{\text{sol}}$  values are not of local origin (i.e., from harbour activities).

### 3.5 The June–July 2008 event: size segregated chemical composition

Figure 8 shows the particle size distribution derived from multi-stage impactor sampling. The size distribution of the main markers of HFO combustion emissions and crustal elements for the first day of the described event (20 June 2008) and for 17 May 2008, characterized by a high crustal content, are shown. The backward trajectories of 17 May computed over 24 h, shows that the air mass originated from North Africa.

As expected, V and Ni in the HFO combustion event display a maximum in the finest mode (diameter  $< 0.4 \mu\text{m}$ ). Conversely, their concentrations peak at larger size ( $1.1\text{--}2.1 \mu\text{m}$  for Ni, and  $0.4\text{--}0.7 \mu\text{m}$  for V) during the Saharan dust event.

The sulphate distribution shows a monomodal distribution peaked in the  $0.4\text{--}0.7 \mu\text{m}$  fraction during the HFO combustion event, due to the main secondary source. On 17 May sulphate displays a bimodal distribution with a second mode ( $1.1\text{--}2.1 \mu\text{m}$ ) related to its primary sources from Saharan dust and sea spray.

Al and Fe are considered typical markers of the crustal source and are mainly present in the coarse mode on 17 May. During the HFO combustion event their distributions are shifted towards fine particles, suggesting that also the anthropic source may contribute to the occurrence of these elements. The presence of a fine mode also on 17 May suggest the presence of mixed source in the selected event.

It must be noticed that even if for Ni and V we report here the pH 1.5 soluble fraction, and the solubility is different for the two aerosol sources, their concentrations are higher in the HFO combustion event than during the Saharan dust case. The situation is different for the crustal markers. Al shows higher concentrations in the Saharan dust event, while Fe concentrations are higher in the HFO combustion case. Part of this behaviour is due to the different solubility of Fe of different origin. In Saharan dust aerosol Fe is associated with the silicate matrix, or present as oxides, and these compounds are not soluble in the applied conditions ( $\text{HNO}_3$ - pH 1.5). In  $\text{PM}_{10}$  samples collected at Lampedusa  $\text{Fe}_{\text{sol}}$  is generally less than 10 % of the total Fe. On the contrary, the Fe solubility is high for anthropic sources, due to the presence of  $\text{Fe}^0$  or Fe- idroxides, both soluble in  $\text{HNO}_3$ .

### 3.6 Heavy oil combustion contribution to the total aerosol load

By using specific markers of different sources and applying receptor models it is possible to quantify the mass contribution of a specific source to the total PM (Gordon, 1988). Emission factors from different marine vessels and engines and other heavy oil combustion sources can provide insightful information to aid source apportionment studies even if the ratios between the selected markers change from the

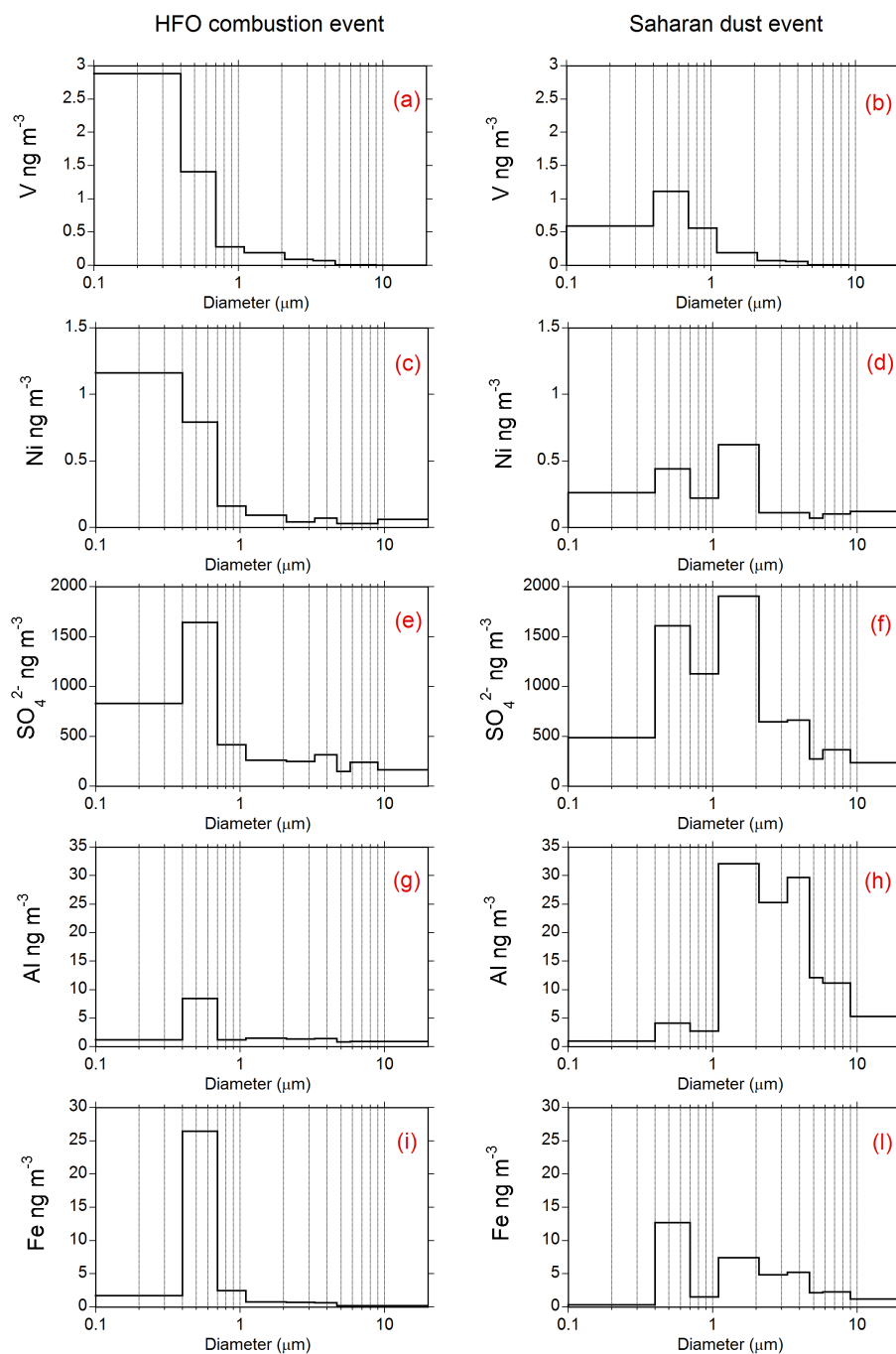


**Fig. 8.**  $V_{\text{sol}}$ ,  $Ni_{\text{sol}}$ ,  $SO_4^{2-}$ ,  $Al_{\text{sol}}$ ,  $Fe_{\text{sol}}$  size distributions during a HFO combustion event (plots on the left, 20 June 2008) and during a Saharan dust event (plot on the right, 17 May 2008).

source to the receptor site for secondary species such as  $nssSO_4^{2-}$ . The main species emitted in the ship plume in gas phase and precursor of particulate are  $NO_x$  and  $SO_2$  (Agrawal et al., 2008a, b). The photochemistry of  $NO_x$  leading to  $NO_3^-$  in the particulate phase is complex, especially in summer (see e.g., Chen et al., 2005), and their contribution to the particulate phase is not here quantified. In this section

the HFO combustion emissions contribution of  $SO_4^{2-}$  to the total amount of  $nssSO_4^{2-}$  and to the PM mass is estimated, considering the ratios between the precursor of particulate in the exhausts of ship engines and V, which is taken as a representative and conservative marker of HFO combustion emission. Agrawal et al. (2008a and b) report average  $SO_4^{2-}/V$  emission ratio of 11–27 in the particulate exhaust ( $PM_{2.5}$ ) of

the main engine of different ocean going container vessels operating at different load. The same authors report higher values (up to about 500) for  $\text{SO}_2(\text{gas})/\text{V}(\text{particulate})$ . However, the amount of  $\text{SO}_4^{2-}$  in the air mass is expected to grow fast due to  $\text{SO}_2$  conversion into sulphate; this conversion is faster in high UV radiation and high humidity conditions.

If we assume an e-folding time of about 2 days for the  $\text{SO}_2$  to  $\text{SO}_4^{2-}$  conversion (Restad et al., 1998), the  $\text{SO}_4^{2-}$  mass is expected to increase by a factor of 10 within 10 h with respect to that contained in the air mass 1 h after the emission. Since the starting  $\text{SO}_4^{2-}/\text{V}$  ratio is in the range 11–27, after 10 h we expect to have a  $\text{SO}_4^{2-}/\text{V}$  ratio of about 110–270. This ratio is expected to vary still more largely, depending on the efficiency of the dry and wet  $\text{SO}_2$  oxidation, and the elapsed time between emission and aerosol sampling. Sulphates originating from processes other than HFO combustion contribute to the total  $\text{SO}_4^{2-}$  load in the collected aerosol, and larger  $\text{SO}_4^{2-}/\text{V}$  ratios may be expected. Figure 4b reports  $\text{nssSO}_4^{2-}$  vs.  $V_{\text{sol}}$  for cases with  $V_{\text{sol}} > 6 \text{ ng m}^{-3}$  (V and Ni enriched events). The crustal contribution to  $\text{nssSO}_4^{2-}$  vs.  $V_{\text{sol}}$  was removed by using typical V/Si and  $\text{SO}_4^{2-}/\text{Si}$  for the upper continental crust (see Sect. 3.1.1; Henderson and Henderson, 2009). Over the whole the data set the  $\text{nssSO}_4^{2-}/V_{\text{sol}}$  ratio is always higher than 200. It must be considered that, once the dust cases have been removed, the addition of  $\text{SO}_4^{2-}$  from sources other than heavy oil combustion would produce (as it appears from figure 4b) an increase in  $\text{SO}_4^{2-}$  without affecting  $V_{\text{sol}}$ . Thus, we assume that the smallest  $\text{SO}_4^{2-}$  to  $V_{\text{sol}}$  ratio may be ascribed to particles in which the contribution from heavy oil combustion is the dominant factor determining sulphate and  $V_{\text{sol}}$  amounts.

For these reason we take  $\text{SO}_4^{2-}/\text{V} = 200$  as a lower limit for particles originating by heavy oil combustion at Lampedusa. In fourteen cases the ratio is close to this limit. Except for two days in March, all cases with  $\text{nssSO}_4^{2-}/\text{V}$  close to 200 occur between May and August. During the special event of June–July 2008 the  $\text{nssSO}_4^{2-}/\text{V}$  ratio values were all in the range 250–400, except for few spikes up to 1000, possibly due to the contribution from additional sources of  $\text{SO}_4^{2-}$ . A value of  $\text{SO}_4^{2-}/\text{V}$  in the same range (285) is derived for the finest particles stage (0.1–0.4  $\mu\text{m}$ ) of the impactor data for the HFO combustion event discussed in Sect. 3.5. Newly formed secondary particles, in this particular event probably arising from ship emissions, are predominantly present in this size range. This is consistent with the findings of Healy et al. (2009 and 2010), who have shown that the majority of freshly emitted ship exhaust particles containing elevated V and sulphate lie in the ultrafine mode (20–600 nm mobility diameter). Larger particles show values of  $\text{SO}_4^{2-}/\text{V} > 400$ , due to an expected stronger contribution of sulphate particles arising from other sources, and the role of coagulation and accretion processes during transport.

By using  $\text{SO}_4^{2-}/\text{V} = 200$  as a lower limit value for HFO combustion emissions in summer, and using the measured values of  $V_{\text{sol}}$  determined at Lampedusa, it is possible to obtain a rough estimation of the minimum contribution of sulphate from the heavy oil combustion source to the total sulphate and total aerosol mass. Due to different meteorological conditions and photochemical activity such a value cannot be applied in general, and to samples collected in different seasons.

For the recognised events the average  $\text{SO}_4^{2-}$  contribution is  $2.12 \mu\text{g m}^{-3}$ , corresponding to 43.6 % of total  $\text{nssSO}_4^{2-}$  mass. This value is higher than the value modelled by Endersen et al. (2003; 2.9 %) which is however an annual global average. The high values we found are likely due the regional (highly affected by ship traffic) and seasonal (late spring–summer) scale here considered. Marmer and Langmann (2005) estimated an average sulphate concentration of  $3.3 \mu\text{g m}^{-3}$  over the Mediterranean basin in summer 2002, with higher values in the Sicily channel. They estimate that ship emissions contribute by 50 % to the total amount of  $\text{nssSO}_4^{2-}$ , and consider the natural contribution negligible. Total  $\text{nssSO}_4^{2-}$  values modelled by Marmer and Langmann (2005) in the summer months (JJA) are in the range  $4.5\text{--}5.2 \mu\text{g m}^{-3}$  over the 2002–2003 period in JJA in the Strait of Sicily, consistent with the measured  $\text{nssSO}_4^{2-}$  average concentration at Lampedusa:  $4.0 \mu\text{g m}^{-3}$  over the 2004–2008 period in JJA. In the same time period the mean  $\text{SO}_4^{2-}$  from HFO combustion computed using the  $V_{\text{sol}}$  content is  $1.2 \mu\text{g m}^{-3}$ , corresponding to about 30 % of the total  $\text{nssSO}_4^{2-}$  content. This percentage is lower than the one modelled by Marmer and Langmann (2005), possibly due to an underestimation of the true  $\text{SO}_4^{2-}/\text{V}$  ratio and/or the underestimation of long range and especially marine biogenic contribution in the model. These results suggest that ship emissions play a large role among the heavy combustion sources in the central Mediterranean.

During the June–July 2008 special event shown in Fig. 7 (26 June 2008) the  $\text{nssSO}_4^{2-}$  from HFO combustion emission reached  $6.1 \mu\text{g m}^{-3}$ , contributing by 15 % to the total  $\text{PM}_{10}$ .

As shown in Sect. 3.5, the HFO combustion aerosols belong mainly the fine particles fraction; by using the average summer V content and mass data obtained at Lampedusa for  $\text{PM}_{2.5}$  and  $\text{PM}_1$  we obtain a contribution of  $\text{SO}_4^{2-}$  from HFO combustion aerosol of about 8 % and 11 %, respectively, in the two aerosol fractions in summer.

#### 4 Conclusions

Daily aerosol samples collected at Lampedusa from 2004 to 2008 were analysed to determine their chemical composition and to identify the possible influence of heavy oil combustion emissions in the central Mediterranean.

Heavy fuel oil combustion events are identified using V and Ni, specific markers of this source. Their ratio to Si is

used to discriminate between crustal and ship sources. The Ni and V soluble fractions are consistently higher for the cases influenced by HFO combustion than for mineral particles.

The V soluble fraction was chosen to identify days affected by high anthropic aerosol content. A threshold of  $6 \text{ ng m}^{-3}$  was established to select heavy oil combustion aerosol events.

A progressive vector analysis based on wind measurements show that the selected events are very likely mainly affected by sea going ship, mainly transiting in the Sicily Channel.

A marked seasonal behaviour, with summer maxima, is observed for all the main HFO combustion aerosol markers ( $V_{\text{sol}}$ ,  $Ni_{\text{sol}}$  and  $nssSO_4^{2-}$ ). The following processes occurring in summer are believed to play an important role in determining the observed seasonal evolution:

1-Increased photochemical activity of atmosphere in summer, leading to a larger production of secondary aerosols, mainly  $nssSO_4^{2-}$

2-MBL stability, higher in summer than winter, that prevents the accumulation of HFO combustion emission compounds in the lowest atmospheric levels in winter.

The higher occurrence of late spring-summer episodes lasting more than one day in correspondence with dominant wind direction from the Sicily Channel, suggests that ship emissions contribute significantly to the heavy oil combustion aerosols.

A very intense event in spring 2008 was studied. Size segregated chemical analyses show that elements arising from heavy oil combustion (V and Ni, but also Al and Fe) are mainly distributed in the sub-micrometric fraction of the aerosol. The metals are present as free metals, carbonates, oxides hydrates or labile complex with organic ligands, so that they are dissolved in mild condition ( $HNO_3$ , pH1.5).

The  $SO_4^{2-}/V$  ratio of 200 is proposed as lower limit characteristic ratio for HFO combustion in summer at Lampedusa. The experimental determination of a characteristic ratio of HFO combustion markers in a receptor site is particularly useful for understanding and quantifying the profile emission.

Between the components emitted by HFO combustion,  $SO_4^{2-}$  contributes significantly to the total PM mass. In summer the estimated average mass is  $1.2 \mu\text{g m}^{-3}$ , about 30 % of the total  $nssSO_4^{2-}$ , 3.9 % of  $PM_{10}$ , 8 %  $PM_{2.5}$ , and 11 %  $PM_1$ . Sulphate from HFO combustion reach a peak value of  $6.1 \mu\text{g m}^{-3}$  on 26 June 2008, corresponding to 47 % of  $nssSO_4^{2-}$ , and 15 % of  $PM_{10}$ . It has to be emphasized we used a conservative value for the  $SO_4^{2-}/V$  ratio which is expected to produce a lower limit of the HFO combustion-derived sulphates, whose contribution may be higher than derived here.

For future studies, more data on size resolved chemical composition (including other pollutants emitted in the ship

plume, e.g. organic and elemental carbon) from sites located in the open sea can provide a better evaluation of the regional and global impact of ship aerosols on the total aerosol budget and on climate.

*Acknowledgements.* The study has been partially supported by the Italian Ministry for University and Research through the SNUMMASS and the Aeroclouds Projects.

Edited by: M. C. Facchini

## References

- Adams, F. C., Van Craen, M. J., and Van Espen P. J.: Enrichment of trace elements in remote aerosols, *Environ. Sci. Technol.*, 14, 1002–1005, 1980.
- Agrawal, H., Malloy, Q., Welch, W. A., Miller, J. W., and Cocker D. R.: In-use gaseous and particulate matter emissions from a modern oceangoing container vessel, *Atmos. Environ.*, 42, 5504–5510, doi:10.1016/j.atmosenv.2008.02.053, 2008a.
- Agrawal, H., Welch, W. A., Miller, J. W., and Cocker D. R.: Emission measurements from a crude oil tanker at sea, *Environ. Sci. Technol.*, 42, 7098–7103, doi:10.1021/es703102y, 2008b.
- Agrawal, H., Welch, W. A., Henningsen, S., Miller, J. W., and Cocker III, D. R.: Emissions from main propulsion engine on container ship at sea, *J. Geophys. Res.*, 115, D23205, doi:10.1029/2009JD013346, 2010.
- Amato, F., Pandolfi, M., Escrig, A., Querol, X., Alastuey, A., Pey, J., Perez, N., and Hopke, P. K.: Quantifying road dust resuspension in urban environment by multilinear engine: a comparison with PMF2, *Atmos. Environ.*, 43, 2770–2780, 2009.
- Artuso, F., Chamard, P., Piacentino, S., Sferlazzo, D. M., De Silvestri, L., di Sarra, A., Meloni, D., Monteleone F.: Influence of transport and trends in atmospheric  $CO_2$  at Lampedusa, *Atmos. Environ.*, 43, 3044–3051, 2009.
- Artuso, F., Chamard, P., Chiavarini, S., di Sarra, A., Meloni, D., Piacentino, S. and Sferlazzo, D. M.: Tropospheric halocarbons and nitrous oxide monitored at a remote site in the Mediterranean, *Atmos. Environ.*, 44, 4944–4953, 2010.
- Ault, A. P., Gaston, C. J., Wang, Y., Dominguez, G., Thiemens, M. H., and Prather, K. A.: Characterization of the single particle mixing state of individual ship plume events measured at the port of Los Angeles, *Environ. Sci. Technol.*, 44, 1954–1961, 2010.
- Barbu, A. L., Segers, A. J., Schaap, M., Heemink, A. W., and Builtjes, P. J. H.: A multi-component data assimilation experiment directed to sulphur dioxide and sulphate over Europe, *Atmos. Environ.*, 43, 1622–1631, 2009.
- Becagli, S., Ghedini, C., Peeters, S., Rottiers, A., Traversi, R., Udisti, R., Chiari, M., Jalba, A., Despiou, S., Dayan, U., and Temara, A.: MBAS (Methylene Blue Active Substances) and LAS (Linear Alkylbenzene Sulphonates) in Mediterranean coastal aerosols: sources and transport processes, *Atmos. Environ.*, 45, 6788–6801, 2011.
- Calzolari G., Chiari, M., García Orellana, I., Lucarelli, F., Migliori, A., Nava, S., and Taccetti, F.: The new external beam facility for environmental studies at the Tandatron accelerator of LABEC, *Nucl. Instr. Meth. B*, 249, 928–931, 2006.
- Casasanta, G., di Sarra, A., Meloni, D., Monteleone, F., Pace, G., Piacentino, S., and Sferlazzo, D.: Large aerosol effects on ozone

- photolysis in the Mediterranean, *Atmos. Environ.*, 45, 3937–3943, 2011.
- Chen, G., Huey, L. G., Trainer, M., Nicks, D., Corbett, J., Ryerson, T., Parrish, D., Neuman, J. A., Nowak, J., Tanner, D., Holloway, J., Brock, C., Crawford, J., Oslon, J. R., Sullivan, A., Weber, R., Schauffler, S., Donnelly, S., Altas, E., Roberts, J., Flocke, F., Hübler, G., and Fehsenfeld, F.: An investigation of the chemistry of ship emission plumes during ITCT 2002, *J. Geophys. Res.*, 110, D10S90, doi:10.1029/2004JD005236, 2005.
- Chester, R., Nimmo, M., Fones, G. R., Keyse, S., and Zhang, Z.: Trace metal chemistry of particulate aerosols from the UK mainland coastal rim of the NE Irish sea, *Atmos. Environ.*, 34, 949–958, 2000.
- Coakley Jr., J. A. and Walsh, C. D.: Limits to the aerosol indirect radiative effect derived from observations of ship tracks, *J. Atmos. Sci.*, 59, 668–680, 2002.
- Cofala, J., Amann, M., Hayes, C., Wagner, F., Klimont, Z., Posch, M., Schopp, W., Tarrason, N., Jonson, J. E., Whall, C., and Stavrakaki, A.: Analysis of policy measures to reduce ship emissions in the context of the revision of national emission ceilings directive. International Institute for Applied Systems Analysis (IIASA), IIASA contract no. 06-107, 2007.
- Conover, J. H.: Anomalous cloud lines, *J. Atmos. Sci.*, 23, 778–785, 1966.
- Corbett, J. J., Winebrake, J. J., Green, E. H., Kasibhatla, P., Eyring, V., and Lauer, A.: Mortality from Ship Emissions: A Global Assessment, *Environ. Sci., Technol.*, 41, 8512–8518, doi:10.1021/es071686z, 2007.
- Dayan, U., Heffter, J. L., and Miller J. M.: Meteorological and climatological data from surface and upper measurements for the assessment of atmospheric transport and deposition of pollutants in the Mediterranean Basin: Part B: Seasonal distribution of the planetary boundary layer depths over the Mediterranean Basin, UNEP Mediterranean Action Plan Technical Reports Series no. 30, Athens, Greece, 1989.
- Derwent, R., Stevenson, D. S., Doherty, R. M., Collins, W. J., Sanderson, M. G., Amann, M., and Dentener, F.: The contribution from ship emissions to air quality and acid deposition in Europe, *Ambio*, 34, 54–59, 2005.
- Devasthale, A., Krüger, O., and Graßl, H.: Impact of ship emissions on cloud properties over coastal areas, *Geophys. Res. Lett.*, 33, L02811, doi:10.1029/2005GL024470, 2006.
- Di Biagio, C., di Sarra, A., and Meloni, D.: Large atmospheric shortwave radiative forcing by Mediterranean aerosol derived from simultaneous ground-based and spaceborne observations, and dependence on the aerosol type and single scattering albedo, *J. Geophys. Res.*, 115, D10209, doi:10.1029/2009JD012697, 2010.
- Di Iorio T., di Sarra, A., Sferlazzo, D. M., Cacciani, M., Meloni, D., Monteleone, F., Fuà, D., and Fiocco G.: Seasonal evolution of the tropospheric aerosol vertical profile in the central Mediterranean and role of desert dust, *J. Geophys. Res.* 114, D02201, doi:10.1029/2008JD010593, 2009.
- di Sarra, A., Cacciani, M., Chamard, P., Cornwall, C., DeLuisi, J. J., Di Iorio, T., Disterhoft, P., Fiocco, G., Fuà, D., and Monteleone, F.: Effects of desert dust and ozone on the ultraviolet irradiance at the Mediterranean island of Lampedusa during PAUR II, *J. Geophys. Res.*, 107, 8135, doi:10.1029/2000JD000139, 2002.
- di Sarra, A., Di Biagio, C., Meloni, D., Monteleone, F., Pace, G., Pugnaghi, S., and Sferlazzo, D.: Shortwave and longwave radiative effects of the intense Saharan dust event of 25–26 March, 2010, at Lampedusa (Mediterranean sea), *J. Geophys. Res.*, 116, D23209, doi:10.1029/2011JD016238, 2011.
- Draxler, R. R. and Rolph, G. D.: HYSPLIT (HYbrid Single-Particle Lagrangian Integrated Trajectory) Model access via NOAA ARL READY Website <http://ready.arl.noaa.gov/HYSPLIT.php>, NOAA Air Resources Laboratory, Silver Spring, MD, USA, 2012.
- Endresen, Ø., Sørgård, E., Sundet, J. K., Dalsøren, S. B., Isaksen, I. S. A., Berglen, T. F., and Gravir, G.: Emissions from international sea transportation and environmental impact, *J. Geophys. Res.*, 108, 4560, doi:10.1029/2002JD002898, 2003.
- Eyring, V., Koehler, H. W., van Aardenne, J., and Lauer, A.: Emissions from international shipping: 1. The last 50 years, *J. Geophys. Res.*, 110, D17305, doi:10.1029/2004JD005619, 2005.
- Gaffney, J. S. and Marley, N. A.: The impacts of combustion emission on air quality and climate – From coal to biofuels and beyond, *Atmos. Environ.*, 43, 26–36, 2009.
- Gordon, G. E.: Receptor models, *Environ. Sci. Technol.*, 22, 1132–1142, 1988.
- Healy, R. M., O'Connor, I. P., Hellebust, S., Allanic, A., Sodeau, J. R., and Wenger, J. C.: Characterisation of single particles from in-port ship emissions, *Atmos. Environ.*, 43, 6408–6414, 2009.
- Healy, R. M., Hellebust, S., Kourtchev, I., Allanic, A., O'Connor, I. P., Bell, J. M., Healy, D. A., Sodeau, J. R., and Wenger, J. C.: Source apportionment of PM<sub>2.5</sub> in Cork Harbour, Ireland using a combination of single particle mass spectrometry and quantitative semi-continuous measurements, *Atmos. Chem. Phys.*, 10, 9593–9613, doi:10.5194/acp-10-9593-2010, 2010.
- Harrison, L., Michalsky, J., and Berndt, J.: Automated multifilter rotating shadowband radiometer: an instrument for optical depth and radiation measurements, *Appl. Opt.*, 33, 5118–5125, 1994.
- Henderson, P. and Henderson, G. M.: Earth science data, Cambridge University Press, 42–44, 2009.
- IMO: IMO Newsroom, Press Briefings, Briefing 46, 10 October 2008, available at: [http://www.imo.org/Newsroom/mainframe.asp?topic\\_id=1709&docid=10262](http://www.imo.org/Newsroom/mainframe.asp?topic_id=1709&docid=10262), 2008.
- Jonson, J. E., Tarrason, L., Klein, H., Vestreng, V., Cofala, J., and Whall, C.: Effects of ship emissions on European ground-level ozone in 2020, *Int. J. Remote Sens.*, 30, 4099–4110, 2009.
- Koçak, M., Mihalopoulos, N., and Kubilay, N.: Contribution of natural source to high PM<sub>10</sub> and PM<sub>2.5</sub> events in the eastern Mediterranean, *Atmos. Environ.*, 41, 3806–3818, 2007.
- Kouvarakis, G., Tsigaridis, K., Kanakidou, M., and Mihalopoulos, N.: Temporal variations of surface regional background ozone over Crete Island in the southeast Mediterranean, *J. Geophys. Res.*, 105, 4399–4407, 2000.
- Lack, D., Corbett, J. J., Onasch, T., Lerner, B., Massoli, P., Quinn, P. K., Bates, T. S., Covert, D. S., Coffman, D., Sierau, B., Herndon, S., Allan, J., Baynard, T., Lovejoy, E., Ravishankara, A. R., and Williams, E.: Particulate emissions from commercial shipping: Chemical, physical, and optical properties, *Geophys. Res. Lett.*, 114, D00F04, doi:10.1029/2008JD011300, 2009.
- Lauer, A., Eyring, V., Hendricks, J., Jöckel, P., and Lohmann, U.: Global model simulations of the impact of ocean-going ships on aerosols, clouds, and the radiation budget, *Atmos. Chem. Phys.*, 7, 5061–5079, doi:10.5194/acp-7-5061-2007, 2007.

- Lelieveld, J. and Dentener, F. J.: What controls tropospheric ozone?, *J. Geophys. Res.*, 105, 3531–3551, 2000.
- Li, Z. and Aneja, V. P.: Regional analysis of cloud chemistry at high elevations in the eastern United States, *Atmos. Environ.*, 26A, 2001–2017, 1992.
- Lucarelli, F., Nava, S., Calzolari, G., Chiari, M., Udisti, R., and Marino, F.: Is PIXE still a useful technique for the analysis of atmospheric aerosols? The LABEC experience, *X-Ray Spectrometry*, 40, 162–167, 2011.
- Mamanea, Y., Perrino, C., Yossefa, O., and Catrambone, M.: Source characterization of fine and coarse particles at the East Mediterranean coast, *Atmos. Environ.*, 42, 6114–6130, 2008.
- Marmer, E. and Langmann, B.: Impact of ship emissions on Mediterranean summertime pollution and climate: A regional model study, *Atmos. Environ.*, 39, 4659–4669, 2005.
- Marmer, E., Dentener, F., Aardenne, J. v., Cavalli, F., Vignati, E., Velchev, K., Hjorth, J., Boersma, F., Vinken, G., Mihalopoulos, N., and Raes, F.: What can we learn about ship emission inventories from measurements of air pollutants over the Mediterranean Sea?, *Atmos. Chem. Phys.*, 9, 6815–6831, doi:10.5194/acp-9-6815-2009, 2009.
- Mazzei F., D'Alessandro, A., Lucarelli, F., Nava, S., Prati, P., Valli, G., and Vecchi R.: Characterization of particulate matter sources in an urban environment. *Sci. of Tot. Environ.*, 401, 81–89, 2008.
- Meloni, D., di Sarra, A., Di Iorio, T., and Fiocco G.: Direct radiative forcing of Saharan dust in the Mediterranean from measurements at Lampedusa island and MISR space-borne observations, *J. Geophys. Res.*, 109, D08206, doi:10.1029/2003JD003960, 2004.
- Meloni, D., di Sarra, A., Pace, G. and Montealeone, F.: Optical properties of aerosols over the central Mediterranean. 2. Determination of single scattering albedo at two wavelengths for different aerosol types, *Atmos. Chem. Phys.*, 6, 715–727, doi:10.5194/acp-6-715-2006, 2006.
- Meloni, D., di Sarra, A., Biavati, G., DeLuisi, J. J., Montealeone, F., Pace, G., Piacentino, S., and Sferlazzo, D.: Seasonal behavior of Saharan dust events at the Mediterranean island of Lampedusa in the period 1999–2005, *Atmos. Environ.*, 41, 3041–3056, doi:10.1016/j.atmosenv.2006.12.001, 2007.
- Moldanova, J., Fridell, E., Popovicheva, O., Demirdjian, B., Tishkova, V., Faccinnetto, A., and Focsa, C.: Characterization of particulate matter and gaseous emissions from a large ship diesel engine, *Atmos. Environ.*, 43, 2632–2641, doi:10.1016/j.atmosenv.2009.02.008, 2009.
- Nicolás, J., Chiari, M., Crespo, J., Orellana, I. G., Lucarelli, F., Nava, S., Pastor, C., and Yubero, E.: Quantification of Saharan and local dust impact in an arid Mediterranean area by the positive matrix factorization (PMF) technique, *Atmos. Environ.*, 42, 8872–8882, 2008.
- Nigam, A., Welch, W., Wayne Miller, J., and Cocher III, D. R.: Effect of fuel sulphur content and control technology on PM emission from ship's auxiliary engine. Proceeding international aerosol conference, St. Paul, USA, 10–15 September 2006, 1531–1532, 2006.
- Olivier, J. G. J., Van Aardenne, J. A., Dentener, F., Pagliari, V., Ganzeveld, L. N., and Peters, J. A. H. W.: Recent trends in global greenhouse gas emissions: regional trends 1970–2000 and spatial distribution of key sources in 2000, *Environ. Sci.*, 2, 81–99, doi:10.1080/15693430500400345, 2005.
- ORTC (Observatoire Régional des Transports de la Corse): Les trafics passagers de la Corse au cours de la saison 2011, available at: [www.ortc.info](http://www.ortc.info), 2011.
- Pace, G., di Sarra, A., Meloni, D., Piacentino, S., and Chamard, P.: Aerosol optical properties at Lampedusa (Central Mediterranean). 1. Influence of transport and identification of different aerosol types, *Atmos. Chem. Phys.*, 6, 697–713, doi:10.5194/acp-6-697-2006, 2006.
- Pandolfi, M., Gonzalez-Castanedo, Y., Alastuey, A., da la Rosa, J.D., Mantilla, E., de la Campa, A.S., Querol X., Pey J., Amato F., Moreno T.: Source apportionment of PM<sub>10</sub> and PM<sub>2.5</sub> at multiple sites in the strait of Gibraltar by PMF: impact of shipping emissions, *Environ. Sci. Pollut. Res.*, 18, 260–269, 2011.
- Petzold, A., Hasselbach, J., Lauer, P., Baumann, R., Franke, K., Gurk, C., Schlager, H. and Weingartner, E.: Experimental studies on particle emissions from cruising ship, their characteristic properties, transformation and atmospheric lifetime in the marine boundary layer, *Atmos. Chem. Phys.*, 8, 2387–2403, doi:10.5194/acp-8-2387-2008, 2008.
- Remoundaki, E., Bourliva, A., P. Kokkalis, Mamouri, R.E., Papayannis, A., Grigoratos, T., Samara, C., and Tsezos, M.: PM<sub>10</sub> composition during an intense Saharan dust transport event over Athens (Greece), *Sci. Total Environ.*, 409, 4361–4372, 2011.
- Restad, K., Isaksen, I. S. A., and Berntsen, T. K.: Global distribution of sulfate in the troposphere: A three-dimensional model study, *Atmos. Environ.*, 32, 3593–3609, 1998.
- Rolph, G. D.: Real-time Environmental Applications and Display sYstem (READY) Website, <http://ready.arl.noaa.gov>, NOAA Air Resources Laboratory, Silver Spring, MD, USA, 2012.
- Sippula, O., Hokkinen, J., Puustinen, H., Yli-Pirilä, P., and Jokiniemi J.: Comparison of particle emissions from small heavy fuel oil and wood-fired boilers. *Atmos. Environ.*, 43, 4855–4864, 2009.
- Song, C. H., Chen, G., and Davis, D. D.: Chemical evolution and dispersion of ship plumes in the remote marine boundary layer: investigation of sulfur chemistry, *Atmos Environ.*, 37, 2663–2679, 2003.
- Stern, N.: Stern Review on the Economics of Climate Change, HMTreasury, The Stationary Office, London, UK, 2007.
- Tzannatos, E.: Ship emissions and their externalities for Greece, *Atmos. Environ.*, 44, 2194–2202, 2010.
- Vestreng, V., Mareckova, K., Kakareka, S., Malchykhina, A., and Kukharchyk, T.: Inventory Review 2007; Emission Data reported to LRTAP Convention and NEC Directive, MSC-W Technical Report 1/07, The Norwegian Meteorological Institute, Oslo, Norway, 2007.
- Viana, M., Amato, F., Alastuey, A., Querol, X., Saúl, G., Hecce-Garraleta, D., and Fernandez-Patier, R.: Chemical tracers of particulate emissions from commercial shipping, *Environ Sci Technol* 43, 7472–7477, 2009.